

DNA hypermethylation of aurora kinase A in hepatitis C virus-positive hepatocellular carcinoma

ZUOHONG MA, YEFU LIU, ZHIQIANG HAO, XIANGDONG HUA and WENXIN LI

Department of Hepatopancreatobiliary Surgery, Cancer Hospital of China Medical University, Shenyang, Liaoning 110042, P.R. China

Received October 1, 2018; Accepted March 5, 2019

DOI: 10.3892/mmr.2019.10487

Abstract. Changes in the methylation levels of tumor suppressor genes or proto-oncogenes are involved in the pathogenesis of hepatitis C virus (HCV) infection-induced hepatocellular carcinoma (HCC). The aim of the present study was to identify novel aberrantly methylated differentially expressed genes by integrating mRNA expression profile (GSE19665 and GSE62232) and methylation profile (GSE60753) microarrays downloaded from the Gene Expression Omnibus database. Functional enrichment analysis of screened genes was performed using the DAVID software and BinGO database. Protein-protein interaction (PPI) networks were constructed using the STRING database, followed by module analysis with MCODE software. The transcriptional and translational expression levels of crucial genes were confirmed using The Cancer Genome Atlas (TCGA) datasets and Human Protein Atlas database (HPA). A total of 122 downregulated/hypermethylated genes and 63 upregulated/hypomethylated genes were identified. These genes were enriched in the Gene Ontology biological processes terms of 'inflammatory response' [Fos proto-oncogene, AP-1 transcription factor subunit (FOS)] and 'cell cycle process' [aurora kinase A (AURKA), cyclin dependent kinase inhibitor 3 (CDKN3) and ubiquitin conjugating enzyme E2 C (UBE2C)]. PPI network and module analysis indicated that human oncogenes FOS, AURKA, CDKN3 and UBE2C may be hub genes. mRNA, protein expression and methylation levels of AURKA and FOS were validated by TCGA and HPA data. In conclusion, aberrantly methylated AURKA and FOS may be potential therapeutic targets for HCV-positive HCC.

Introduction

Hepatocellular carcinoma (HCC) is a common malignancy and the leading cause of cancer-related mortality, with an estimated 42,220 new cases diagnosed and 30,200 mortalities in the United States in 2018 (1). Despite curative surgical resection and recent advances in adjuvant chemotherapy, radiotherapy and liver transplantation, recurrence and metastasis occur frequently, leading to the overall 5-year survival rate <20% (2). Although multiple factors have been linked to the development and progression of HCC, hepatitis virus infection is considered to be the predominant underlying cause. It has been reported that the burden of HCC parallels the prevalence of hepatitis C virus (HCV) (3). The 10-year survival rate was reported to be approximately 35% in HCC patients with HCV (4). Thus, it is necessary to explore the molecular mechanisms of HCV-associated hepatocarcinogenesis to screen novel prognostic biomarkers and to develop effective therapeutic strategies.

Although the mechanism of the pathogenesis by which HCV induces HCC is currently unclear, epigenetic changes (such as DNA methylation) have been demonstrated to serve fundamental roles. For example, aberrant hypermethylation of tumor suppressor genes or hypomethylation of proto-oncogenes may result in the decrease or increase in their expression levels and induce excessive proliferation, migration and invasion of hepatocytes (5). Methylation of several genes has been reported in HCV-associated HCC (6). For example, Ramadan *et al* demonstrated that the frequency of aberrant methylation in the promoter region of serine protease inhibitor kunitz-type 2 gene was significantly higher in HCV-positive HCC cases compared with HCV-positive cirrhosis and normal control patients (7). Takagi *et al* reported that CpG islands in zygote arrest 1 exon 1 had a higher methylation level in HCV-positive HCC compared with non-tumorous tissues (8). Tsunedomi *et al* not only demonstrated a correlation between DNA methylation and mRNA expression levels of ATP-binding cassette subfamily B member 6 (ABCB6), but also revealed that aberrant mRNA and DNA methylation levels of ABCB6 may serve as predictive biomarkers for early intrahepatic recurrence of HCV-positive HCC (9). *In vitro* studies by Mileo *et al* (10) and Quan *et al* (11) demonstrated that HCV may promote the progression of HCC cells by downregulating the protein and mRNA levels of proline rich protein BstNI

Correspondence to: Dr Xiangdong Hua, Department of Hepatopancreatobiliary Surgery, Cancer Hospital of China Medical University, 44 Xiaoheyuan Road, Dadong, Shenyang, Liaoning 110042, P.R. China
E-mail: xdh20927@sohu.com

Key words: hepatocellular carcinoma, hepatitis C virus, methylation, differentially expressed genes, bioinformatics, aurora kinase A

subfamily 2/p130 and secreted frizzled-related protein, a Wnt antagonist, by inducing promoter hypermethylation. However, genes with aberrant DNA methylation for HCV-positive HCC remain largely under-investigated.

The aim of the present study was to identify novel genes to explain the development of HCV-positive HCC by combining mRNA expression profile and methylation profile microarrays, and to confirm their transcriptional and translational expression using The Cancer Genome Atlas (TCGA) datasets and Human Protein Atlas database (HPA). The results of the present study may provide novel therapeutic targets for HCV-positive HCC.

Materials and methods

Microarray data collection. Three microarray datasets: GSE19665 (12), GSE62232 (13) and GSE60753 (14) were downloaded from the Gene Expression Omnibus database (<http://www.ncbi.nlm.nih.gov/geo>) on July 25, 2018. The GSE19665 dataset [platform, GPL570 Affymetrix Human Genome U133 Plus 2.0 Array (HG-U133_Plus_2)] was used to analyze the gene expression profile in 20 HCC and 20 matched non-cancerous tissues, among which 5 pairs were HCV-positive; the GSE62232 dataset (platform, HG-U133_Plus_2) was used to detect the gene expression profile in 81 HCC (including 9 HCV-positive) and 10 normal liver tissues; and the GSE60753 dataset (platform, GPL13534, Illumina HumanMethylation450 BeadChip) was used to determine the DNA methylation profile in 156 HCC (including 12 HCV-positive), 34 normal liver tissues and 1 HCC cell line. Normal liver tissues were not matched with HCC in GSE62232 and GSE60753, but only collected from patients without HCC (such as benign cysts). Only the HCV-positive HCC and normal control samples were used for our following analyses.

Microarray data preprocessing. For the GSE19665 and GSE62232 datasets, the raw data were preprocessed using the oligo package (version 1.42.0; <http://www.bioconductor.org/packages/release/bioc/html/oligo.html>) in Bioconductor R package (version 3.4.1; <http://www.R-project.org>), including data transformation, missing value imputation with median, background correction with microarray analysis suite method and quantile normalization. For the GSE60753 dataset, the DNA methylation β values were downloaded and the genes were annotated according to the annotation information from the corresponding platform.

Differential gene expression and methylation analysis. Differentially expressed genes (DEGs) and differentially methylated genes (DMGs) between HCV-positive HCC and control samples were identified using the Linear Models for Microarray Data method (version 3.34.0; <https://bioconductor.org/packages/release/bioc/html/limma.html>) (15) in the Bioconductor R package. False discovery rate (FDR) <0.05 and $\log_2(\text{FC}) > 1$ were defined as the statistical threshold value; where FC is fold change. Hierarchical clustering (16) was performed for the DEGs and DMGs using pheatmap R package (version 1.0.8; <https://cran.r-project.org/web/packages/pheatmap/>) based on Euclidean distance and the results were displayed as a heat map. The upregulated and downregulated shared DEGs in GSE19665 and GSE62232 datasets were

then overlapped with the hypomethylated and hypermethylated DMGs, respectively, to identify the methylated-mediated genes. Additionally, the methylated-mediated genes were compared with the human oncogenes downloaded from the ONGene database (<http://ongene.bioinfo-minzhao.org>) (17) to screen for HCC-related oncogenes.

Protein-protein interaction (PPI) network construction and module analysis. The STRING database (version 10.0; <http://string-db.org>) (18) was used to predict the interactions between DEGs, and a PPI network was constructed using the obtained interaction pairs using the Cytoscape software (version 3.6.1; <http://www.cytoscape.org>) (19). The topological characteristics of the nodes (proteins) in the PPI network were computed using the CytoNCA plugin in the Cytoscape software (<http://apps.cytoscape.org/apps/cytonca>) (20) to determine the hub genes, including 'degree' [the number of edges (interactions) of a node (protein)], 'betweenness' (the number of shortest paths that run through a node), 'closeness centrality' (CC; the average length of the shortest paths to access all other proteins in the network) and 'average path length' (APL; the average distance between all pairs of nodes). Functionally related modules with well-interconnected genes were further identified in the PPI network using the Molecular Complex Detection (MCODE; version 1.4.2; <http://apps.cytoscape.org/apps/mcode>) algorithm (21) with the following scoring options: Degree cutoff=2; node score cutoff=0.2; K-core=2. Modules with MCODE score (Density*Nodes) >3 and node number >6 were considered to be significant.

Function enrichment analysis. Gene Ontology (GO) biological process terms and Kyoto Encyclopedia of Genes and Genomes (KEGG) pathway enrichment analyses were performed for the methylated-mediated DEGs using the Database for Annotation, Visualization and Integrated Discovery (DAVID) online tool (version 6.8; <http://david.abcc.ncifcrf.gov>) (22) and BinGO (23) plugin in Cytoscape to predict their underlying functions. Statistical significance was defined as $P < 0.05$ or FDR <0.05.

Validation of the selected methylation-mediated DEGs. The mRNA and methylation sequencing data of HCC tissues and normal liver tissues from patients without HCC were extracted from TCGA database (<https://portal.gdc.cancer.gov>) prior to July 25, 2018, which were measured on the Illumina HiSeq 2000 RNA Sequencing platform. Only the HCV-positive HCC samples were included in the present study to confirm the expression consistency of the methylated-mediated DEGs. The expression difference between HCC and controls was determined by Student's independent t-test using the TCGA data. $P < 0.05$ was considered to indicate a statistically significant difference.

In addition, protein expression levels of the methylated-mediated DEGs were also validated by the HPA database (version 18; <https://www.proteinatlas.org>) (24), which was used to evaluate the translational levels of the DEGs by immunohistochemistry. Results are presented as the sum of scores of staining intensity (negative, weak, moderate or strong) and the percentage of stained cells (<25, 25-75 or >75%): Negative-not

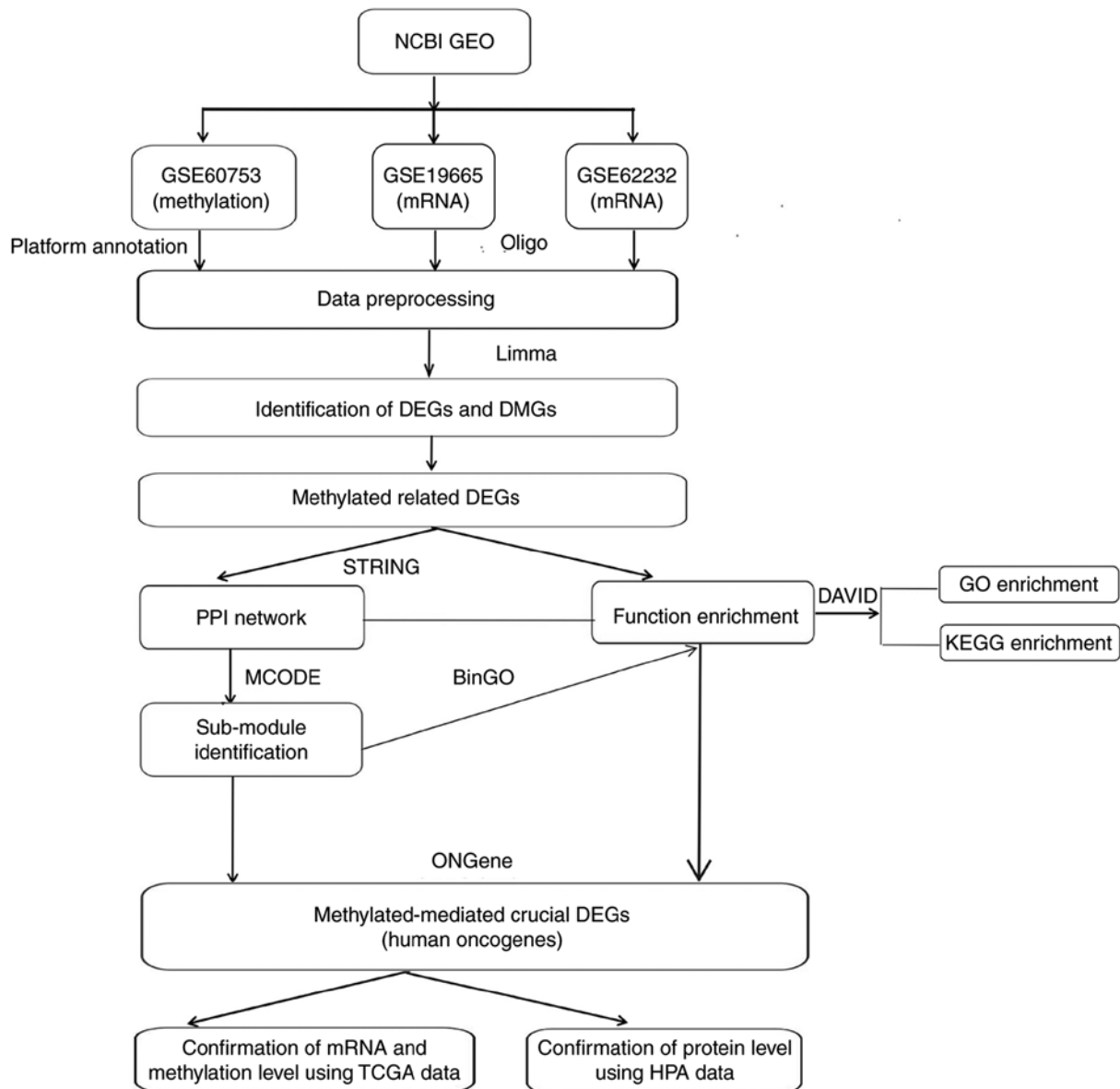


Figure 1. Analysis plan. The key genes were determined by integrating the methylation and mRNA expression profile microarray datasets and then confirmed using TCGA and HPA data. DAVID, Database for Annotation, Visualization and Integrated Discovery; DEGs, differentially expressed genes; DMGs, differentially methylated genes; GEO, Gene Expression Omnibus; GO, Gene Ontology; HPA, Human Protein Atlas; KEGG, Kyoto Encyclopedia of Genes and Genomes; limma, Linear Models for Microarray Data; PPI, protein-protein interaction; TCGA, The Cancer Genome Atlas.

detected; weak + <25%-not detected; weak + 25-75 or 75%-low; moderate <25%-low; moderate + 25-75 or 75%-medium; strong <25%-medium, strong + 25-75 or 75%-high.

Results

Differential gene expression and methylation. A flowchart depicting the analytical process is presented as Fig. 1. Following preprocessing, a total of 1,306 (735 downregulated and 571 upregulated) and 1,249 (330 downregulated and 919 upregulated) DEGs were identified between HCV-positive HCC and control tissues in GSE19665 and GSE62232 datasets, respectively, using the cut-off criteria $FDR < 0.05$ and $|\log FCI| > 1$. The hierarchical-clustering heat map (Fig. 2A and B) indicated that DEGs may be used to distinguish HCV-positive HCC from control samples.

A total of 23,408 methylated probes were annotated to genes in the GSE60753 dataset. By comparing with normal samples, 1,448 DMGs (903 hypomethylated and 545 hypermethylated) were also obtained in HCV-positive HCC tissues. The hierarchical-clustering heat map (Fig. 2C) revealed that DMGs were different between HCV-positive HCC and control samples.

Following comparison of the DEGs identified in GSE19665 and GSE62232 datasets, 173 downregulated and 278 upregulated DEGs were revealed to be common and their expression trends were consistent in the two datasets (Fig. 3A). Further integration with the DMGs found 122 DEGs were downregulated by DNA hypermethylation and 63 DEGs were upregulated by DNA hypomethylation (Fig. 3B). Among the methylated DEGs, nine were suggested as human oncogenes according to the prediction by ONGene database;

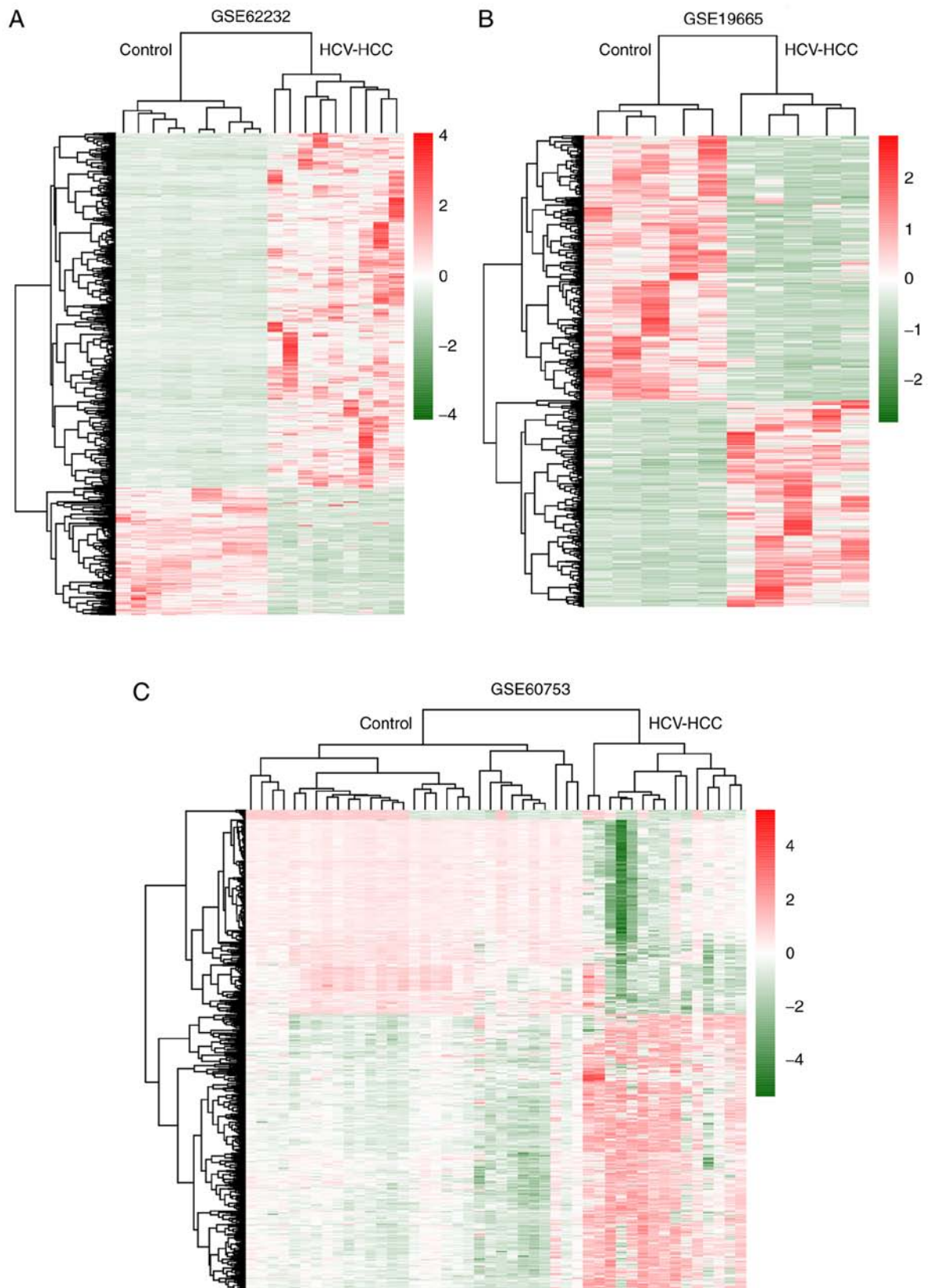


Figure 2. Differentially expressed and methylated genes in HCV-positive HCC. (A-C) Hierarchical clustering and heat map analysis of differentially expressed genes in (A) GSE19665 and (B) GSE62232 and of (C) differentially methylated genes in GSE60753. Red, high expression (or hypermethylation); green, low expression (or hypomethylation). HCC hepatocellular carcinoma; HCV, hepatitis C virus.

five were downregulated: Inhibitor of DNA binding 1, HLH protein (ID1), epithelial cell adhesion molecule (EPCAM),

Fos proto-oncogene, AP-1 transcription factor subunit (FOS), ID2 and placenta specific 8 (PLAC8), whereas four

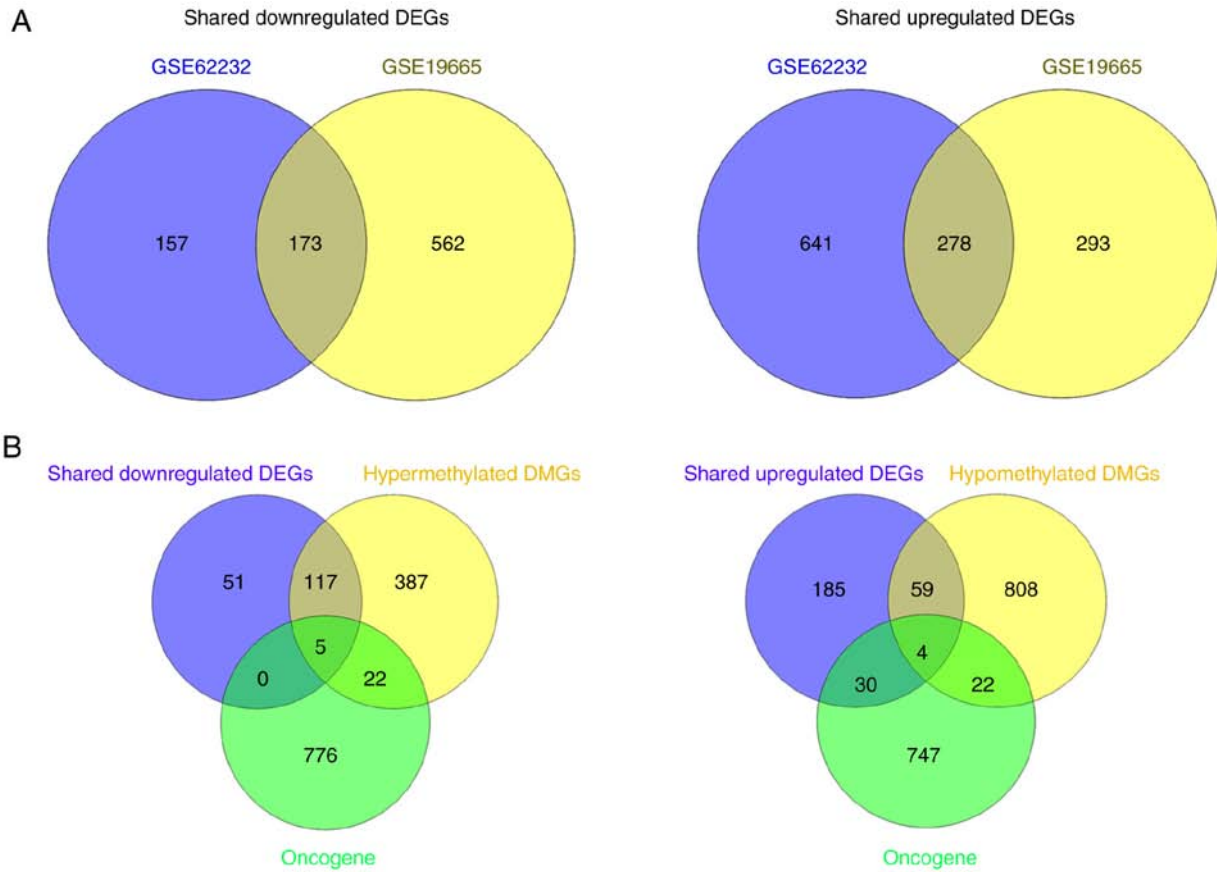


Figure 3. Shared DEGs in GSE19665 and GSE62232 hepatitis C virus-positive hepatocellular carcinoma datasets. (A and B) Venn diagrams demonstrate (A) shared DEGs in GSE19665 and GSE62232 and (B) their association with DMGs in GSE60753. DEGs, differentially expressed genes; DMGs, differentially methylated genes.

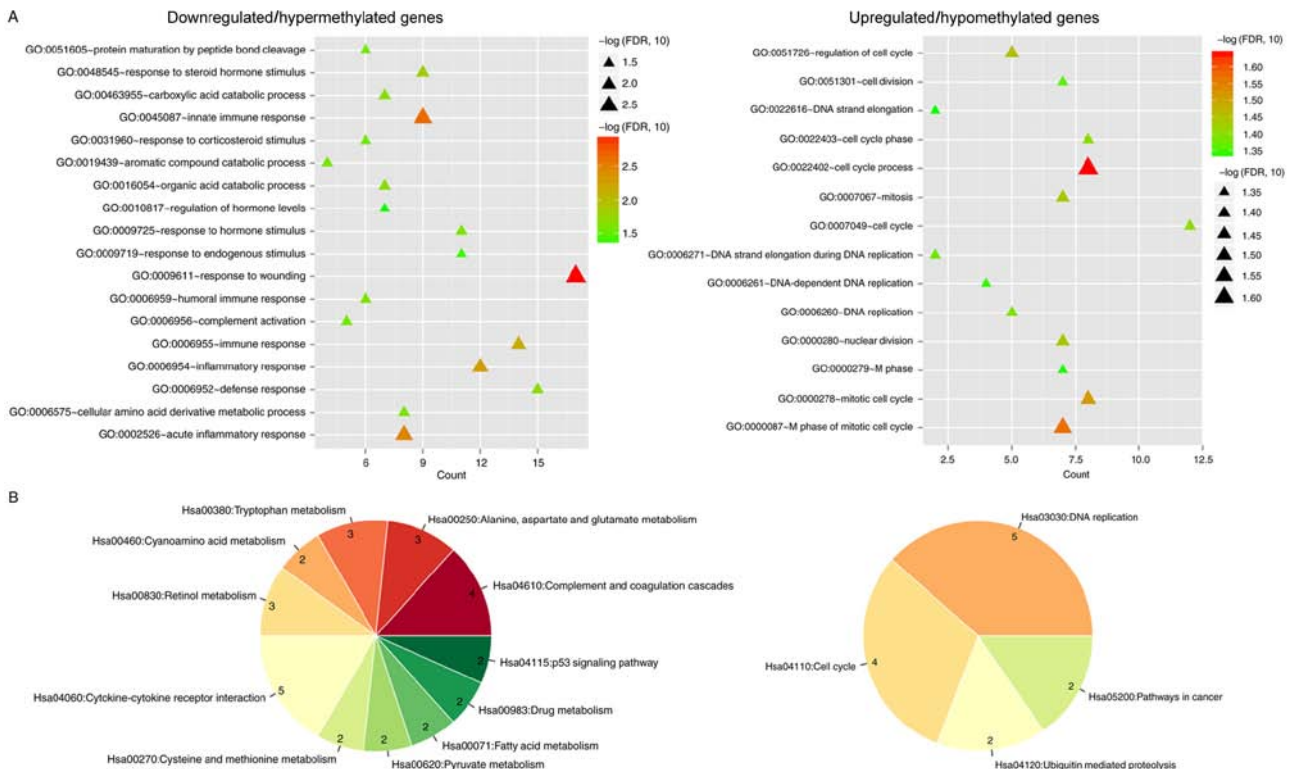


Figure 4. GO and KEGG enrichment analyses of the methylation-related DEGs. (A) GO biological process term analysis. Triangles indicate the significance level (P-value adjusted to FDR). (B) KEGG pathway enrichment. Left, downregulated/hypermethylated DEGs; right, upregulated/hypomethylated DEGs. DEGs, differentially expressed genes; FDR, false discovery rate; GO, Gene Ontology; KEGG, Kyoto Encyclopedia of Genes and Genomes.

Table I. GO enrichment for methylation-related differentially expressed genes.

A, Downregulated/hypermethylated genes			
GO ID	GO term	FDR	Genes
0051605	Protein maturation by peptide bond cleavage	2.87x10 ⁻²	CFP, C8B, C7, FCN3, KLKB1, C1R
0048545	Response to steroid hormone stimulus	1.47x10 ⁻²	PRSS8, FOS, GOT1, CCL2, ACADS, WFDC1, CA2, NPY1R, GHR
0046395	Carboxylic acid catabolic process	2.18x10 ⁻²	ASPA, GOT1, ACADS, IDO2, KMO, UROC1, PON3
0045087	Innate immune response	2.26x10 ⁻³	CFP, C8B, C7, FCN3, IL1RAP, VNN1, C1R, CD1D, GCH1
0031960	Response to corticosteroid stimulus	2.93x10 ⁻²	PRSS8, FOS, GOT1, CCL2, ACADS, GHR
0019439	Aromatic compound catabolic process	2.70x10 ⁻²	EPHX2, IDO2, KMO, PON3
0016054	Organic acid catabolic process	2.18x10 ⁻²	ASPA, GOT1, ACADS, IDO2, KMO, UROC1, PON3
0010817	Regulation of hormone levels	4.64x10 ⁻²	ALDH8A1, SHBG, LY6E, CRHBP, CYP26A1, SRD5A1, BCO2
0009725	Response to hormone stimulus	2.54x10 ⁻²	PRSS8, FOS, GOT1, CCL2, HMGCS2, ACADS, FBP1, WFDC1, CA2, NPY1R, GHR
0009719	Response to endogenous stimulus	4.10x10 ⁻²	PRSS8, FOS, GOT1, CCL2, HMGCS2, ACADS, FBP1, WFDC1, CA2, NPY1R, GHR
0009611	Response to wounding	1.02x10 ⁻³	C7, CCL2, HPS5, EPHX2, CHST4, C1R, CFP, C8B, FOS, LPA, PLSCR4, FCN3, KLKB1, IL1RAP, PROZ, VNN1, NGFR
0006959	Humoral immune response	2.46x10 ⁻²	CFP, C8B, C7, CCL2, FCN3, C1R
0006956	Complement activation	2.70x10 ⁻²	CFP, C8B, C7, FCN3, C1R
0006955	Immune response	6.96x10 ⁻³	C7, CCL2, CHST4, C1R, VIPR1, CXCL12, CD1D, GCH1, CFP, C8B, FCN3, HAMP, IL1RAP, VNN1
0006954	Inflammatory response	5.26x10 ⁻³	CFP, C8B, FOS, C7, CCL2, FCN3, KLKB1, IL1RAP, EPHX2, VNN1, C1R, CHST4
0006952	Defense response	1.98x10 ⁻²	C7, CCL2, EPHX2, CHST4, C1R, CD1D, GCH1, CFP, C8B, FOS, FCN3, HAMP, KLKB1, IL1RAP, VNN1
0006575	Cellular amino acid derivative metabolic process	2.47x10 ⁻²	GGT5, LY6E, IDO2, VNN1, KMO, BBOX1, GHR, GCH1
0002526	Acute inflammatory response	3.37x10 ⁻³	CFP, C8B, C7, FCN3, KLKB1, EPHX2, VNN1, C1R
B, Upregulated/hypomethylated genes			
GO ID	GO term	FDR	Genes
0051726	Regulation of cell cycle	3.52x10 ⁻²	TP53BP2, NUSAP1, SFN, CDKN3, UBE2C
0051301	Cell division	4.37x10 ⁻²	RAD21, NUSAP1, NDC80, PARD3B, CEP55, UBE2C, CDCA3
0022616	DNA strand elongation	4.65x10 ⁻²	RFC4, FEN1
0022403	Cell cycle phase	3.99x10 ⁻²	RAD21, NUSAP1, NDC80, AURKA, CEP55, CDKN3, UBE2C, CDCA3
0022402	Cell cycle process	2.27x10 ⁻²	RAD21, NUSAP1, NDC80, AURKA, CEP55, CDKN3, UBE2C, CDCA3
0007067	Mitosis	3.63x10 ⁻²	RAD21, NUSAP1, NDC80, AURKA, CEP55, UBE2C, CDCA3
0007049	Cell cycle	3.98x10 ⁻²	RAD21, TP53BP2, E2F8, NUSAP1, NDC80, AURKA, PARD3B, CEP55, CDKN3, UBE2C, CDCA3, MCM6
0006271	DNA strand elongation during DNA replication	4.22x10 ⁻²	RFC4, FEN1
0006261	DNA-dependent DNA replication	4.56x10 ⁻²	RFC4, MCM4, FEN1, MCM6
0006260	DNA replication	4.15x10 ⁻²	RFC4, RNASEH2A, MCM4, FEN1, MCM6

Table I. Continued.

B, Upregulated/hypomethylated genes			
GO ID	GO term	FDR	Genes
000028	Nuclear division	3.63x10 ⁻²	RAD21, NUSAP1, NDC80, AURKA, CEP55, UBE2C, CDCA3
0000279	M phase	4.61x10 ⁻²	RAD21, NUSAP1, NDC80, AURKA, CEP55, UBE2C, CDCA3
0000278	Mitotic cell cycle	3.06x10 ⁻²	RAD21, NUSAP1, NDC80, AURKA, CEP55, CDKN3, UBE2C, CDCA3
0000087	M phase of mitotic cell cycle	2.68x10 ⁻²	RAD21, NUSAP1, NDC80, AURKA, CEP55, UBE2C, CDCA3

FDR, false discovery rate; GO, Gene Ontology.

Table II. KEGG pathway enrichment for methylation-related differentially expressed genes.

A, Downregulated/hypermethylated genes			
KEGG ID	KEGG pathway	P-value	Genes
hsa04610	Complement and coagulation cascades	3.13x10 ⁻³	C8B, C7, KLKB1, C1R
hsa00250	Alanine, aspartate and glutamate metabolism	3.81x10 ⁻³	ASPA, GOT1, ASS1
hsa00380	Tryptophan metabolism	6.04x10 ⁻³	AADAT, IDO2, KMO
hsa00460	Cyanoamino acid metabolism	6.82x10 ⁻³	GBA3, GGT5
hsa00830	Retinol metabolism	1.02x10 ⁻²	CYP4A11, CYP26A1, RDH16
hsa04060	Cytokine-cytokine receptor interaction	2.67x10 ⁻²	CCL2, IL1RAP, NGFR, CXCL12, GHR
hsa00270	Cysteine and methionine metabolism	2.91x10 ⁻²	GOT1, BHMT
hsa00620	Pyruvate metabolism	3.33x10 ⁻²	LDHD, ACOT12
hsa00071	Fatty acid metabolism	3.33x10 ⁻²	CYP4A11, ACADS
hsa00983	Drug metabolism	3.53x10 ⁻²	NAT2, UPP2
hsa04115	p53 signaling pathway	4.98x10 ⁻²	GADD45B, IGFBP3

B, Upregulated/hypomethylated genes			
hsa03030	DNA replication	1.70x10 ⁻⁵	RFC4, RNASEH2A, MCM4, FEN1, MCM6
hsa04110	Cell cycle	1.79x10 ⁻²	RAD21, SFN, MCM4, MCM6
hsa04120	Ubiquitin mediated proteolysis	4.67x10 ⁻²	UBE2C, UBE2Q1
hsa05200	Pathways in cancer	4.79x10 ⁻²	LAMC1, CTNNA1

KEGG, Kyoto Encyclopedia of Genes and Genomes.

were upregulated: Aurora kinase A (AURKA), ubiquitin conjugating enzyme E2 C (UBE2C), erb-b2 receptor tyrosine kinase 3 (ERBB3) and cyclin-dependent kinase inhibitor 3 (CDKN3).

Functional enrichment for the DEGs. The 122 downregulated/hypermethylated and 63 upregulated/hypomethylated DEGs were respectively uploaded to DAVID to predict their functions. Using the threshold value of FDR <0.05, 18 GO biological process terms were obtained for the downregulated/hypermethylated DEGs, including ‘response

to wounding’ (FOS) and ‘inflammatory response’ (FOS), whereas 14 GO biological process terms were enriched for the upregulated/hypomethylated DEGs, including ‘cell cycle process’ (AURKA, CDKN3 and UBE2C) and ‘cell cycle’ (CDKN3 and MCM6) (Fig. 4A; Table I). Furthermore, KEGG pathway enrichment analysis was also performed, which resulted in 11 KEGG pathways identified as enriched for downregulated/hypermethylated and 4 enriched for upregulated/hypomethylated DEGs, using the threshold value of P<0.05 (FDR >0.05 for all pathways) (Fig. 4B; Table II). The KEGG pathway enrichment results were consistent with

Table III. Top 15 genes based on each topological characteristic.

Node	Degree	Node	Closeness centrality	Node	Average path length	Node	Betweenness Centrality
NDC80	18	FAT1	1.00	FAT1	1.00	FAT1	1.00
CDKN3 ^a	16	SMAD5	1.00	SMAD5	1.00	FOS	0.52
AURKA ^a	16	CBFA2T3	1.00	CBFA2T3	1.00	CDKN3 ^a	0.40
UBE2C ^a	15	SPP2	1.00	SPP2	1.00	FEN1	0.36
NUSAP1	15	FNIP1	1.00	FNIP1	1.00	MTR	0.35
RFC4	14	WFDC1	1.00	WFDC1	1.00	LPL	0.25
KIF4A	14	ECM1	1.00	ECM1	1.00	LPA	0.18
CEP55	14	SLC22A1	1.00	SLC22A1	1.00	IGFBP3	0.17
FEN1	13	SLC10A1	1.00	SLC10A1	1.00	TXNRD1	0.16
ATAD2	13	ID1	1.00	ID1	1.00	SHBG	0.16
MCM4	13	RRAGD	1.00	RRAGD	1.00	ASS1	0.16
FOS	11	CTNNA1	0.67	CTNNA1	1.50	CCL2	0.15
MCM6	11	LAMC1	0.67	LAMC1	1.50	ACADS	0.15
RNASEH2A	11	CDKN3 ^a	0.28	FOS	3.54	APOF	0.14
DEPDC1	8	FOS	0.28	CDKN3 ^a	3.54	CANX	0.14

^aPotential hub gene.

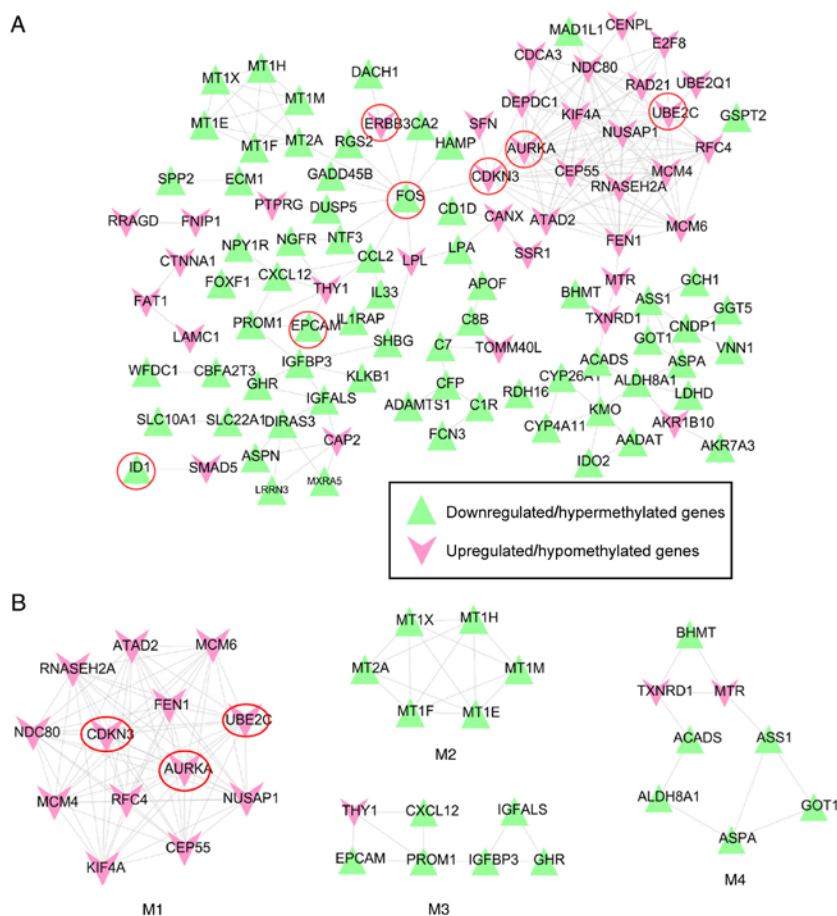


Figure 5. PPI network of the methylation-related differentially expressed genes. (A) An overall PPI network constructed using the protein interaction data from the STRING 10.0 database. (B) Functional highly connected sub-modules extracted from the PPI network using the Molecular Complex Detection plugin of Cytoscape software. Red, upregulated genes; green, downregulated genes; circled genes are known human oncogenes. AURKA, aurora kinase A; CDKN3, cyclin-dependent kinase inhibitor 3; EPCAM, epithelial cell adhesion molecule; ERBB3, erb-b2 receptor tyrosine kinase 3; FOS, Fos proto-oncogene, AP-1 transcription factor subunit; ID1, inhibitor of DNA binding 1, HLH protein; M1, module 1; M2, module 2; M3, module 3; M4, module 4; PPI, protein-protein interaction; UBE2C, ubiquitin conjugating enzyme E2 C.

Table IV. GO enrichment for genes in modules.

A, Module 1			
GO ID	P _{corr}	GO term	Genes in test set
48015	1.86x10 ⁻⁶	Phosphoinositide-mediated signaling	FEN1, RFC4, UBE2C, NDC80, AURKA
278	3.01x10 ⁻⁵	Mitotic cell cycle	UBE2C, NUSAP1, NDC80, CEP55, AURKA, CDKN3
6260	3.01x10 ⁻⁵	DNA replication	FEN1, RNASEH2A, RFC4, MCM4, MCM6
22403	3.65x10 ⁻⁵	Cell cycle phase	UBE2C, NUSAP1, NDC80, CEP55, AURKA, CDKN3
280	3.65x10 ⁻⁵	Nuclear division	UBE2C, NUSAP1, NDC80, CEP55, AURKA
7067	3.65x10 ⁻⁵	mitosis	UBE2C, NUSAP1, NDC80, CEP55, AURKA
87	3.65x10 ⁻⁵	M phase of mitotic cell cycle	UBE2C, NUSAP1, NDC80, CEP55, AURKA
7049	4.09x10 ⁻⁵	Cell cycle	UBE2C, NUSAP1, MCM6, NDC80, CEP55, AURKA, CDKN3
51301	1.03x10 ⁻⁴	Cell division	UBE2C, NUSAP1, NDC80, CEP55, AURKA
22402	1.03x10 ⁻⁴	Cell cycle process	UBE2C, NUSAP1, NDC8, CEP55, AURKA, CDKN3
279	1.35x10 ⁻⁴	M phase	UBE2C, NUSAP1, NDC80, CEP55, AURKA
35556	4.36x10 ⁻³	Intracellular signal transduction	FEN1, RFC4, UBE2C, NDC80, AURKA
6996	5.42x10 ⁻³	Organelle organization	UBE2C, KIF4A, NUSAP1, NDC80, CEP55, AURKA
34645	1.06x10 ⁻²	Cellular macromolecule biosynthetic process	FEN1, RNASEH2A, RFC4, MCM4, MCM6
9059	1.08x10 ⁻²	Macromolecule biosynthetic process	FEN1, RNASEH2A, RFC4, MCM4, MCM6
23034	1.41x10 ⁻²	Intracellular signaling pathway	FEN1, RFC4, UBE2C, NDC80, AURKA
90304	2.84x10 ⁻²	Nucleic acid metabolic process	FEN1, RNASEH2A, RFC4, MCM4, MCM6
44249	4.55x10 ⁻²	Cellular biosynthetic process	FEN1, RNASEH2A, RFC4, MCM4, MCM6

B, Module 2

GO ID	P _{corr}	GO term	Genes in test set
10273	9.41x10 ⁻³	Detoxification of copper ion	MT2A
10038	9.41x10 ⁻³	Response to metal ion	MT2A, MT1X
10035	1.12x10 ⁻²	Response to inorganic substance	MT2A, MT1X
6882	1.12x10 ⁻²	Cellular zinc ion homeostasis	MT2A
55069	1.12x10 ⁻²	Zinc ion homeostasis	MT2A
6878	1.12x10 ⁻²	Cellular copper ion homeostasis	MT2A
55070	1.12x10 ⁻²	Copper ion homeostasis	MT2A
7263	1.37x10 ⁻²	Nitric oxide mediated signal transduction	MT2A
46688	1.48x10 ⁻²	Response to copper ion	MT2A

C, Module 3

GO ID	P _{corr}	GO term	Genes in test set
30334	1.28x10 ⁻²	Regulation of cell migration	CXCL12, IGFBP3, THY1
51270	1.28x10 ⁻²	Regulation of cellular component movement	CXCL12, IGFBP3, THY1
40012	1.28x10 ⁻²	Regulation of locomotion	CXCL12, IGFBP3, THY1
42325	3.08x10 ⁻²	Regulation of phosphorylation	GHR, IGFBP3, THY1
19220	3.08x10 ⁻²	Regulation of phosphate metabolic process	GHR, IGFBP3, THY1
51174	3.08x10 ⁻²	Regulation of phosphorus metabolic process	GHR, IGFBP3, THY1
45595	3.08x10 ⁻²	Regulation of cell differentiation	GHR, IGFBP3, THY1
7155	3.56x10 ⁻²	Cell adhesion	CXCL12, THY1, IGFBP3

Table IV. GO enrichment for genes in modules.

C, Module 3			
GO ID	P _{corr}	GO term	Genes in test set
22610	3.56x10 ⁻²	Biological adhesion	CXCL12, THY1, IGFALS
32879	3.64x10 ⁻²	Regulation of localization	CXCL12, IGFBP3, THY1
50793	3.69x10 ⁻²	Regulation of developmental process	GHR, IGFBP3, THY1
48522	3.81x10 ⁻²	Positive regulation of cellular process	GHR, CXCL12, IGFBP3, THY1
48518	4.28x10 ⁻²	Positive regulation of biological process	GHR, CXCL12, IGFBP3, THY1
51239	4.29x10 ⁻²	Regulation of multicellular organismal process	GHR, IGFBP3, THY1
10646	4.53x10 ⁻²	Regulation of cell communication	GHR, IGFBP3, THY1
7166	4.93x10 ⁻²	Cell surface receptor linked signaling pathway	GHR, CXCL12, THY1
D, Module 4			
GO ID	P _{corr}	GO term	Genes in test set
19752	7.81x10 ⁻⁸	Carboxylic acid metabolic process	BHMT, GOT1, MTR, ALDH8A1, ACADS, ASPA, ASS1
43436	7.81x10 ⁻⁸	Oxoacid metabolic process	BHMT, GOT1, MTR, ALDH8A1, ACADS, ASPA, ASS1
6082	7.81x10 ⁻⁸	Organic acid metabolic process	BHMT, GOT1, MTR, ALDH8A1, ACADS, ASPA, ASS1
42180	7.81x10 ⁻⁸	Cellular ketone metabolic process	BHMT, GOT1, MTR, ALDH8A1, ACADS, ASPA, ASS1
6520	2.23x10 ⁻⁶	Cellular amino acid metabolic process	BHMT, GOT1, MTR, ASPA, ASS1
44106	6.48x10 ⁻⁶	Cellular amine metabolic process	BHMT, GOT1, MTR, ASPA, ASS1
44281	1.21x10 ⁻⁵	Small molecule metabolic process	BHMT, GOT1, MTR, ALDH8A1, ACADS, ASPA, ASS1
6519	1.21x10 ⁻⁵	Cellular amino acid and derivative metabolic process	BHMT, GOT1, MTR, ASPA, ASS1
9308	1.89x10 ⁻⁵	Amine metabolic process	BHMT, GOT1, MTR, ASPA, ASS1
44283	2.33x10 ⁻⁵	Small molecule biosynthetic process	BHMT, GOT1, MTR, ALDH8A1, ASS1
44237	1.82x10 ⁻³	Cellular metabolic process	BHMT, GOT1, TXNRD1, MTR, ALDH8A1, ACADS, ASPA, ASS1
8152	5.73x10 ⁻³	Metabolic process	BHMT, GOT1, TXNRD1, MTR, ALDH8A1, ACADS, ASPA, ASS1
44249	5.73x10 ⁻³	Cellular biosynthetic process	BHMT, GOT1, MTR, ALDH8A1, ASS1
9058	6.30x10 ⁻³	Biosynthetic process	BHMT, GOT1, MTR, ALDH8A1, ASS1
34641	9.55x10 ⁻³	Cellular nitrogen compound metabolic process	BHMT, GOT1, MTR, ASPA, ASS1
6807	1.19x10 ⁻²	Nitrogen compound metabolic process	BHMT, GOT1, MTR, ASPA, ASS1
44238	1.71x10 ⁻²	Primary metabolic process	BHMT, GOT1, MTR, ALDH8A1, ACADS, ASPA, ASS1

GO, Gene Ontology; P_{corr}, corrected P-value.

GO biological process term analysis, in which inflammatory-related 'cytokine-cytokine receptor interaction' pathway was enriched for downregulated/hypermethylated DEGs, and 'DNA replication' and 'cell cycle' were enriched for upregulated/hypomethylated DEGs.

PPI network. The STRING database identified interaction relationships in 105 out of the 185 methylation-related DEGs (68 downregulated and 37 upregulated). The 211 interaction relationship pairs among the DEGs were used to construct

a PPI network (Fig. 5A); seven of the previously identified human oncogenes were included (downregulated, ID1, FOS and EPCAM; upregulated, AURKA, CDKN3, UBE2C and ERBB3), as no interactions with other DEGs were identified for ID2 and PLAC8.

Two human oncogenes, FOS and CDKN3, were indicated as hub genes of the PPI network as they were shared and ranked in the top 15 for 4 topological characteristics (Table III). In addition, AURKA and UBE2C ranked top 5 in 'degree'. ID1 was one of the top 10 genes in 'CC' and 'APL'.

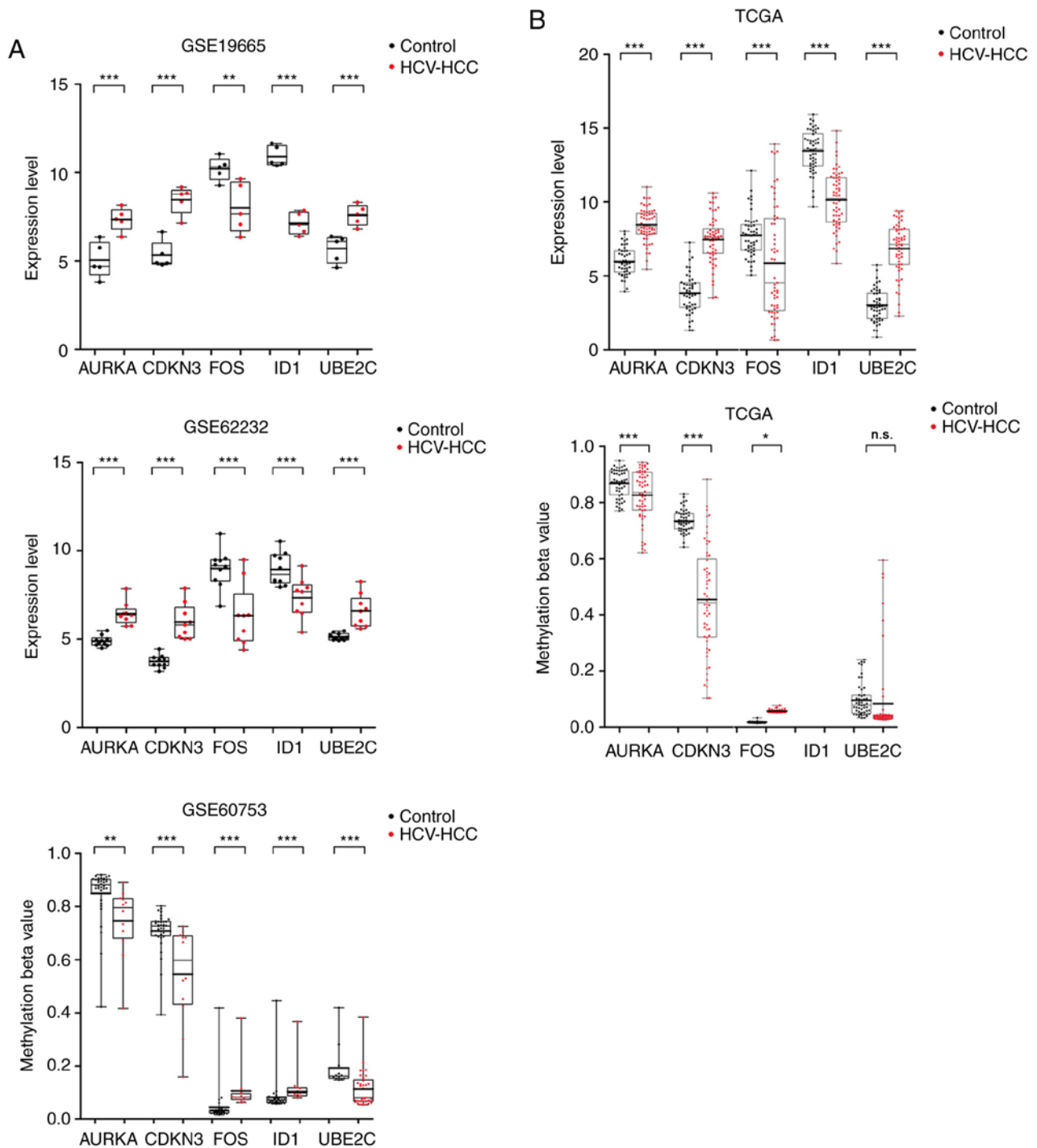


Figure 6. Validation of the hub genes in the samples obtained from TCGA database. (A) Gene expression and methylation levels in samples of microarray datasets GSE19665 (HCV-positive HCC tissues, n=5; normal controls, n=5), GSE62232 (HCV-positive HCC tissues, n=9; normal controls, n=10) and GSE60753 (HCV-positive HCC tissues, n=29; normal controls, n=34). (B) Gene expression and methylation levels in TCGA data (HCV-positive HCC tissues, n=58; normal controls, n=50). Student's independent t-test was used to analyze the differences between HCV-positive HCC and normal controls. * $P < 0.05$, ** $P < 0.01$ and *** $P < 0.001$ vs. control. AURKA, aurora kinase A; CDKN3, and cyclin-dependent kinase inhibitor 3; FOS, Fos proto-oncogene, AP-1 transcription factor subunit; HCC, hepatocellular carcinoma; HCV, hepatitis C virus; ID1, inhibitor of DNA binding 1, HLH protein; UBE2C, ubiquitin conjugating enzyme E2 C; n.s., not significant; TCGA, The Cancer Genome Atlas.

Subsequently, four highly connected PPI sub-modules (Fig. 5B) were extracted from the overall PPI network using MCODE. BinGO enrichment analysis demonstrated that the genes in module 1 (MCODE score=12.81) were involved in mitotic cell cycle (AURKA, CDKN3 and UBE2C); the genes in module 2 (MCODE score=5.067) were associated with detoxification of copper ions; the genes in module 3 (MCODE

score=3.771) participated in the regulation of cell migration; and the genes in module 4 (MCODE score=3.41) were associated with carboxylic acid metabolic process (Table IV).

Validation of the selected methylation-mediated DEGs. Based on the enrichment and PPI analyses, it was hypothesized that downregulated/hypermethylated FOS and ID1 and

upregulated/hypomethylated CDKN3, AURKA and UBE2C may be important human oncogenes for HCV-positive HCC. To further confirm their expression and methylation levels, the mRNA and methylation sequencing data of 58 HCV-HCC tissues and 50 normal controls were obtained from the TCGA database. The results demonstrated that the transcriptional expression and methylation levels of FOS, CDKN3 and AURKA in TCGA sequencing data (Fig. 6B) were consistent with the microarray data (Fig. 6A). However, the methylation level of UBE2C was not significantly different between HCV-positive HCC and normal control TCGA samples, although its expression level was consistent between TCGA sequencing data and our used microarray data (Fig. 6). The methylation level of ID1 had a detection value of 0 in the TCGA and thus comparison was not performed.

In addition, the HPA database was used to confirm the protein expression level of the genes in HCC by immunohistochemistry. Protein expression levels of AURKA in HCC tissues were higher, whereas protein expression levels of FOS in HCC tissues were lower compared with normal hepatocytes (Fig. 7). There was no immunohistochemical result for CDKN3 in the HPA database and no difference was observed in UBE2C and ID1 protein expression levels between HCC and normal control tissues.

Discussion

Through comprehensive analysis and validation, results from the present study indicated that AURKA and FOS may be crucial genes involved in HCV-positive HCC by participating in the cell cycle process and inflammatory response. HCV may upregulate the expression of AURKA and downregulate FOS by changes in DNA methylation.

HCV stimulates excessive cell proliferation in hepatocytes by dysregulating the cell cycle, which induces the development of HCC (25,26). Several positive cell cycle regulators (such as cyclin D1, cyclin E and Rb/p105) have been identified to be upregulated, whereas negative regulators [such as cyclin-dependent kinase 4 (CDK4), CDK6, p21Cip1, p27Kip1 and p57Kip2] are downregulated in patients with HCV-positive HCC compared with patients with chronic hepatitis C with or without liver cirrhosis (27). AURKA, which is located on chromosome 20q13.2, encodes a serine/threonine kinase involved in the assembly and maintenance of the mitotic spindle (28). Thus, AURKA is speculated to be a crucial gene for the regulation of cell cycle and carcinogenesis in several cancer types, including HCC (29). Yang *et al* demonstrated that knockdown of AURKA suppressed the growth of ovarian cancer cells by reducing centrosome amplification, malformation of mitotic spindles, and chromosome aberration (30). Additionally, restoring the expression of p21 and pRb attenuated the effects of AURKA silencing on cell cycle progression (30). Using RNA microarray and reverse transcriptase-quantitative PCR analysis, Zhou *et al* reported that AURKA was significantly upregulated in human urothelial carcinoma compared with normal urothelium (31) and demonstrated that AURKA inhibitor MLN8237 induced cell-cycle arrest, aneuploidy, mitotic spindle failure and apoptosis in human bladder cancer cells, which arrested tumor growth (31). Li *et al* also used the MLN8237 to demonstrate that AURKA regulated cell cycle

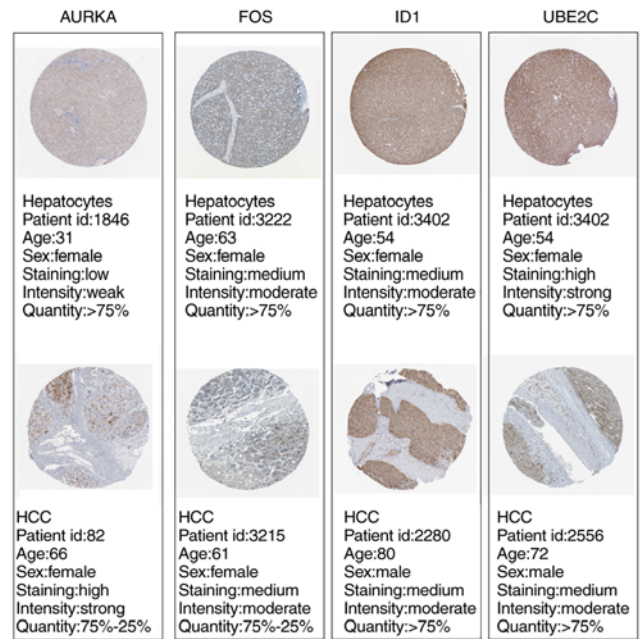


Figure 7. Validation of the hub genes at a translational level using the Human Protein Atlas database. AURKA, aurora kinase A; FOS, Fos proto-oncogene, AP-1 transcription factor subunit; HCC, hepatocellular carcinoma; ID1, inhibitor of DNA binding 1, HLH protein; UBE2C, ubiquitin conjugating enzyme E2 C.

in breast cancer cells by modulating the p53/p21/cell division control 2/cyclin B1 pathway (32). Similarly, the verification experiments demonstrated that AURKA inhibitor alisertib arrested HCC cells in G2/M phase and induced an accumulation of aneuploidy by regulating the expression of key cell cycle regulators such as cyclin B1 (33,34). The present study demonstrated that AURKA was highly expressed at the mRNA and protein levels in HCV-positive HCC. In addition to the cell cycle, a recent study has suggested that AURKA contributes to tumor migration, invasion, epithelial mesenchymal transition and cancer stem cell behaviors, which also have been preliminarily validated in HCC (35), but not HCV-related HCC. Thus, further investigation of the roles of AURKA in HCV-related HCC remains necessary.

DNA methylation is an important mechanism for regulating gene expression epigenetically. Hypermethylation of genes is associated with reduced expression, whereas hypomethylation is associated with increased expression. Thus, high expression of AURKA in HCV-positive HCC was predicted to be due to hypomethylation, which was validated by the microarray and TCGA data. This conclusion agreed with a previous study on esophageal cancer, in which AURKA methylation and human papillomavirus infection was higher in precancer, esophagitis and normal tissues compared with cancer tissues (36). However, further experiments are needed to confirm the effects of HCV on the methylation of AURKA and the development of HCC.

FOS is a member of the fos family of transcription factors, which has been extensively demonstrated to be a pro-oncogenic gene and promote proliferation, invasion and metastasis of cancer through AP-1-related mechanisms, including HCV-positive HCC (37). However, in the present study, FOS was downregulated and hypermethylated. This

may indicate that FOS may be a dual-function gene, which has been identified in other cancers, such as ovarian cancer (38) and pancreatic cancer (39). Alternatively, the results may be negative due to the small sample size. Further studies with larger sample sizes are needed to confirm role of FOS in HCV-positive HCC.

There were certain limitations to the present study. First, although the known microarray and TCGA sequencing data were included to confirm the expression and methylation levels of crucial genes, the sample size associated with HCV-positive HCC was small. Therefore, more clinical samples need to be collected to further confirm their expression levels. Second, although the present study has suggested that the expression levels of AURKA and FOS may be regulated by methylation, additional *in vitro* and *in vivo* experiments using a methylation inhibitor, such as 5-azacytidine, are essential to verify these results. Third, HCV infection-related *in vitro* and *in vivo* experiments (accompanied with overexpression or knockdown of genes) are also needed to demonstrate the functional roles of AURKA and FOS in cell proliferation, apoptosis, migration and invasion.

The results of the present study preliminarily indicate that aberrantly methylated AURKA and FOS may be potential therapeutic targets for treatment of HCV-positive HCC.

Acknowledgements

Not applicable.

Funding

No funding was received.

Availability of data and materials

The sequencing datasets GSE19665 (<https://www.ncbi.nlm.nih.gov/geo/query/acc.cgi?acc=GSE19665>), GSE62232 (<https://www.ncbi.nlm.nih.gov/geo/query/acc.cgi?acc=GSE62232>) and GSE60753 (<https://www.ncbi.nlm.nih.gov/geo/query/acc.cgi?acc=GSE60753>) were downloaded from the GEO database in NCBI. The mRNA and microRNA sequencing data were obtained from The Cancer Genome Atlas (<https://tcga-data.nci.nih.gov>).

Authors' contributions

ZM and XH conceived and designed the study; YL and ZH performed the acquisition of data; ZM and YL conducted the statistical analysis. WL and ZH were involved in the interpretation of the data. ZM drafted the manuscript. XH revised the manuscript. all authors read and approved the final manuscript.

Ethics approval and consent to participate

Not applicable.

Patient consent for publication

Not applicable.

Competing interests

The authors declare that they have no competing interests.

References

1. Siegel RL, Miller KD and Jemal A: Cancer statistics, 2018. *CA Cancer J Clin* 68: 7-30, 2018.
2. Jing L, Huang L, Yan J, Qiu M and Yan Y: Liver resection for hepatocellular carcinoma: Personal experiences in a series of 1330 consecutive cases in China. *ANZ J Surg* 88: E713-E717, 2018.
3. Petruzzello A: Epidemiology of Hepatitis B Virus (HBV) and Hepatitis C Virus (HCV) related hepatocellular carcinoma. *Open Virol J* 12: 26-32, 2018.
4. Moore MS, Bocour A, Tran OC, Qiao B, Schymura MJ, Laraque F and Winters A: Effect of hepatocellular carcinoma on mortality among individuals with Hepatitis B or Hepatitis C infection in New York City, 2001-2012. *Open Forum Infect Dis* 5: ofy144, 2018.
5. Kiran M, Chawla YK and Kaur J: Methylation profiling of tumor suppressor genes and oncogenes in hepatitis virus-related hepatocellular carcinoma in northern India. *Cancer Genet Cytogenet* 195: 112-119, 2009.
6. Zekri AR, Bahnasy AA, Shoeab FE, Mohamed WS, El-Dahshan DH, Ali FT, Sabry GM, Dasgupta N and Daoud SS: Methylation of multiple genes in hepatitis C virus associated hepatocellular carcinoma. *J Adv Res* 5: 27-40, 2014.
7. Ramadan RA, Zaki MA, Awad AM and El-Ghalid LA: Aberrant methylation of promoter region of SPINT2/HAI-2 gene: An epigenetic mechanism in hepatitis C virus-induced hepatocarcinogenesis. *Genet Test Mol Biomarkers* 19: 399-404, 2015.
8. Takagi K, Fujiwara K, Takayama T, Mamiya T, Soma M and Nagase H: DNA hypermethylation of zygote arrest 1 (ZAR1) in hepatitis C virus positive related hepatocellular carcinoma. *Springerplus* 2: 150, 2013.
9. Tsunedomi R, Iizuka N, Yoshimura K, Iida M, Tsutsumi M, Hashimoto N, Kanekiyo S, Sakamoto K, Tamesa T and Oka M: ABCB6 mRNA and DNA methylation levels serve as useful biomarkers for prediction of early intrahepatic recurrence of hepatitis C virus-related hepatocellular carcinoma. *Int J Oncol* 42: 1551-1559, 2013.
10. Mileo AM, Mattarocci S, Matarrese P, Anticoli S, Abbruzzese C, Catone S, Sacco R, Paggi MG and Ruggieri A: Hepatitis C virus core protein modulates pRb2/p130 expression in human hepatocellular carcinoma cell lines through promoter methylation. *J Exp Clin Cancer Res* 34: 140, 2015.
11. Quan H, Zhou F, Nie D, Chen Q, Cai X, Shan X, Zhou Z, Chen K, Huang A, Li S and Tang N: Hepatitis C virus core protein epigenetically silences SFRP1 and enhances HCC aggressiveness by inducing epithelial-mesenchymal transition. *Oncogene* 33: 2826-2835, 2014.
12. Deng YB, Nagae G, Midorikawa Y, Yagi K, Tsutsumi S, Yamamoto S, Hasegawa K, Kokudo N, Aburatani H and Kaneda A: Identification of genes preferentially methylated in hepatitis C virus-related hepatocellular carcinoma. *Cancer Sci* 101: 1501-1510, 2010.
13. Yang Y, Chen L, Gu J, Zhang H, Yuan J, Lian Q, Lv G, Wang S, Wu Y, Yang YC, *et al*: Recurrently deregulated lncRNAs in hepatocellular carcinoma. *Nat Commun* 8: 14421, 2017.
14. Hlady RA, Tiedemann RL, Puszyk W, Zendejas I, Roberts LR, Choi JH, Liu C and Robertson KD: Epigenetic signatures of alcohol abuse and hepatitis infection during human hepatocarcinogenesis. *Oncotarget* 5: 9425-9443, 2014.
15. Ritchie ME, Phipson B, Wu D, Hu Y, Law CW, Shi W and Smyth GK: Limma powers differential expression analyses for RNA-sequencing and microarray studies. *Nucleic Acids Res* 43: e47, 2015.
16. Szekely GJ and Rizzo ML: Hierarchical clustering via Joint between-within distances: Extending Ward's minimum variance method. *J Classification* 22: 151-183, 2005.
17. Liu Y, Sun J and Zhao M: ONGene: A literature-based database for human oncogenes. *J Genet Genomics* 44: 119-121, 2017.
18. Szklarczyk D, Franceschini A, Wyder S, Forslund K, Heller D, Huerta-Cepas J, Simonovic M, Roth A, Santos A, Tsafou KP, *et al*: STRING v10: Protein-protein interaction networks, integrated over the tree of life. *Nucleic Acids Res* 43 (Database Issue): D447-D452, 2015.

19. Kohl M, Wiese S and Warscheid B: Cytoscape: Software for visualization and analysis of biological networks. *Methods Mol Biol* 696: 291-303, 2011.
20. Tang Y, Li M, Wang J, Pan Y and Wu FX: CytoNCA: A cytoscape plugin for centrality analysis and evaluation of protein interaction networks. *Biosystems* 127: 67-72, 2015.
21. Bader GD and Hogue CW: An automated method for finding molecular complexes in large protein interaction networks. *BMC Bioinformatics* 4: 2, 2003.
22. Huang DW, Sherman BT and Lempicki RA: Systematic and integrative analysis of large gene lists using DAVID bioinformatics resources. *Nat Protoc* 4: 44-57, 2009.
23. Maere S, Heymans K and Kuiper M: BiNGO: A Cytoscape plugin to assess overrepresentation of Gene Ontology categories in Biological Networks. *Bioinformatics* 21: 3448-3449, 2005.
24. Pontén F, Jirstrom K and Uhlen M: The human protein atlas-a tool for pathology. *J Pathol* 216: 387-393, 2008.
25. Irshad M, Gupta P and Irshad K: Molecular basis of hepatocellular carcinoma induced by hepatitis C virus infection. *World J Hepatol* 9: 1305-1314, 2017.
26. Moustafa S, Karakasliotis I and Mavromara P: Hepatitis C virus core+1/ARF protein modulates Cyclin D1/pRb pathway and promotes carcinogenesis. *J Virol* 92: pii: e02036-17, 2018.
27. Bassiouny AEE, Nosseir MM, Zoheiry MK, Ameen NA, Abdelhadi AM, Ibrahim IM, Zada S, El-Deen AH and El-Bassiouni NE: Differential expression of cell cycle regulators in HCV-infection and related hepatocellular carcinoma. *World J Hepatol* 2: 32-41, 2010.
28. Kufer TA, Silljé HH, Körner R, Gruss OJ, Meraldi P and Nigg EA: Human TPX2 is required for targeting Aurora-A kinase to the spindle. *J Cell Biol* 158: 617-623, 2002.
29. Benten D, Keller G, Quaas A, Schrader J, Gontarewicz A, Balabanov S, Braig M, Wege H, Moll J, Lohse AW and Brummendorf TH: Aurora kinase inhibitor PHA-739358 suppresses growth of hepatocellular carcinoma in vitro and in a xenograft mouse model. *Neoplasia* 11: 934-944, 2009.
30. Yang G, Chang B, Yang F, Guo X, Cai KQ, Xiao X, Wang H, Sen S, Hung MC, Mills GB, *et al*: Aurora Kinase A promotes ovarian tumorigenesis through dysregulation of the cell cycle and suppression of BRCA2. *Clin Cancer Res* 16: 3171-3181, 2010.
31. Zhou N, Singh K, Mir MC, Parker Y, Lindner D, Dreicer R, Ecsedy JA, Zhang Z, The BT, Almasan A and Hansel DE: The investigational Aurora kinase A inhibitor MLN8237 induces defects in cell viability and cell cycle progression in malignant bladder cancer cells in vitro and in vivo. *Clin Cancer Res* 19: 1717-1728, 2013.
32. Li JP, Yang YX, Liu QL, Pan ST, He ZX, Zhang X, Yang T, Chen XW, Dong W, Qiu JX and Zhou SF: The investigational Aurora kinase A inhibitor alisertib (MLN8237) induces cell cycle G2/M arrest, apoptosis, and autophagy via p38 MAPK and Akt/mTOR signaling pathways in human breast cancer cells. *Drug Des Devel Ther* 9: 1627-1652, 2015.
33. Zhu Q, Yu X, Zhou ZW, Zhou C, Chen XW and Zhou SF: Inhibition of Aurora A Kinase by alisertib induces autophagy and cell cycle arrest and increases chemosensitivity in human hepatocellular carcinoma HepG2 cells. *Curr Cancer Drug Targets* 17: 386-401, 2017.
34. Zhu Q, Yu X, Zhou ZW, Luo M, Zhou C, He ZX, Chen Y and Zhou SF: A quantitative proteomic response of hepatocellular carcinoma Hep3B cells to danusertib, a pan-Aurora kinase inhibitor. *J Cancer* 9: 2061-2071, 2018.
35. Chen C, Song G, Xiang J, Zhang H, Zhao S and Zhan Y: AURKA promotes cancer metastasis by regulating epithelial-mesenchymal transition and cancer stem cell properties in hepatocellular carcinoma. *Biochem Biophys Res Commun* 486: 514-520, 2017.
36. Mohiuddin MK, Chava S, Upendrum P, Latha M, Zubeda S, Kumar A, Ahuja YR, Hasan Q and Mohan V: Role of Human papilloma virus infection and altered methylation of specific genes in esophageal cancer. *Asian Pac J Cancer Prev* 14: 4187-4193, 2013.
37. Watanabe T, Hiasa Y, Tokumoto Y, Hirooka M, Abe M, Ikeda Y, Matsuura B, Chung RT and Onji M: Protein Kinase R modulates c-Fos and c-Jun signaling to promote proliferation of hepatocellular carcinoma with Hepatitis C virus infection. *PLoS One* 8: e67750, 2013.
38. Oliveiraferrer L, Rößler K, Haustein V, Schröder C, Wicklein D, Maltseva D, Khaustova N, Samatov T, Tonevitsky A, Mahner S, *et al*: c-FOS suppresses ovarian cancer progression by changing adhesion. *Br J Cancer* 110: 753-763, 2013.
39. Guo JC, Li J, Zhao YP, Zhou L, Cui QC, Zhou WX, Zhang TP and You L: Expression of c-fos was associated with clinicopathologic characteristics and prognosis in pancreatic cancer. *PLoS One* 10: e0120332, 2015.



This work is licensed under a Creative Commons Attribution-NonCommercial-NoDerivatives 4.0 International (CC BY-NC-ND 4.0) License.